Available online at www.sciencedirect.com
SCIENCE DIRECT®
Precambrian Research 122 (2003) 7–27
Precambrian Research
www.elsevier.com/locate/precamres

Geochemical and Sr–Nd isotopic constraints from the Kontum massif, central Vietnam on the crustal evolution of the Indochina block

Ching-Ying Lan [a,*], Sun-Lin Chung [b], Trinh Van Long [c], Ching-Hua Lo [b], Tung-Yi Lee [d], Stanley A. Mertzman [e], Jason Jiun-San Shen [a]

[a] *Institute of Earth Sciences, Academia Sinica, Nankang, P.O. Box 1-55, Taipei 11529, Taiwan, ROC*
[b] *Department of Geosciences, National Taiwan University, Taipei 106, Taiwan, ROC*
[c] *South Vietnam Geological Mapping Division, Department of Geology and Minerals of Vietnam, Ho Chi Minh City, Viet Nam*
[d] *Department of Earth Sciences, National Taiwan Normal University, Taipei 117, Taiwan, ROC*
[e] *Department of Geosciences, Franklin and Marshall College, Lancaster, PA 17604-3003, USA*

Received 19 December 2001; received in revised form 20 April 2002; accepted 7 July 2002

Abstract

The Kontum massif, central Vietnam, consists mainly of high-grade (amphibolite to granulite facies) metamorphic rocks and represents the largest basement exposure (core complex) of the Indochina block. To explore the crustal evolution of Indochina, Sr and Nd isotopic and geochemical data for various rock types from the massif are reported. The basement rocks show a wide range of present day ε_{Nd} values from −22 (gneiss) to +15 (amphibolite), yielding depleted-mantle model ages (T_{DM}) from 1.2 to 2.4 Ga along with an "exceptionally" old T_{DM} of 2.7 Ga for a granulite. These data indicate that crustal formation in the Indochina block took place principally during the Paleoproterozoic and Mesoproterozoic, and do not support the conventional notion that the Kontum core complex is composed of Archean rocks. Geochemical data indicate that the gneisses and schists have heterogeneous compositions characterized by a calc-alkaline nature, whereas most of the amphibolites are tholeiitic basalts with intraplate magmatic signatures. Therefore, the former may be interpreted as products from pre-existing Proterozoic crustal materials and the latter as resulting from the Paleozoic rifting event that disintegrated the Indochina block from Gondwanaland. During its accretion with other SE Asian continental blocks in Permo-Triassic time, the Indochina core complex was subjected to the Indosinian orogeny, characterized by a high-temperature, granulite facies metamorphism in the lower crust with associated charnockite magmatism and subsequent regional exhumation.

Keywords: Kontum massif; Sr–Nd isotope; Geochemistry; Indochina block; Vietnam

1. Introduction

Southeast Asia consists of allochthonous continental blocks disintegrated from the northern margin of Gondwanaland. These include the South China, Indochina, Sibumasu and West Burma blocks (see inset of Fig. 1), which amalgamated to form the Southeast

* Corresponding author. Tel.: +886-2-27839910x614; fax: +886-2-27839871.
E-mail address: kyanite@earth.sinica.edu.tw (C.-Y. Lan).

0301-9268/02/$ – see front matter
PII: S0301-9268(02)00205-X

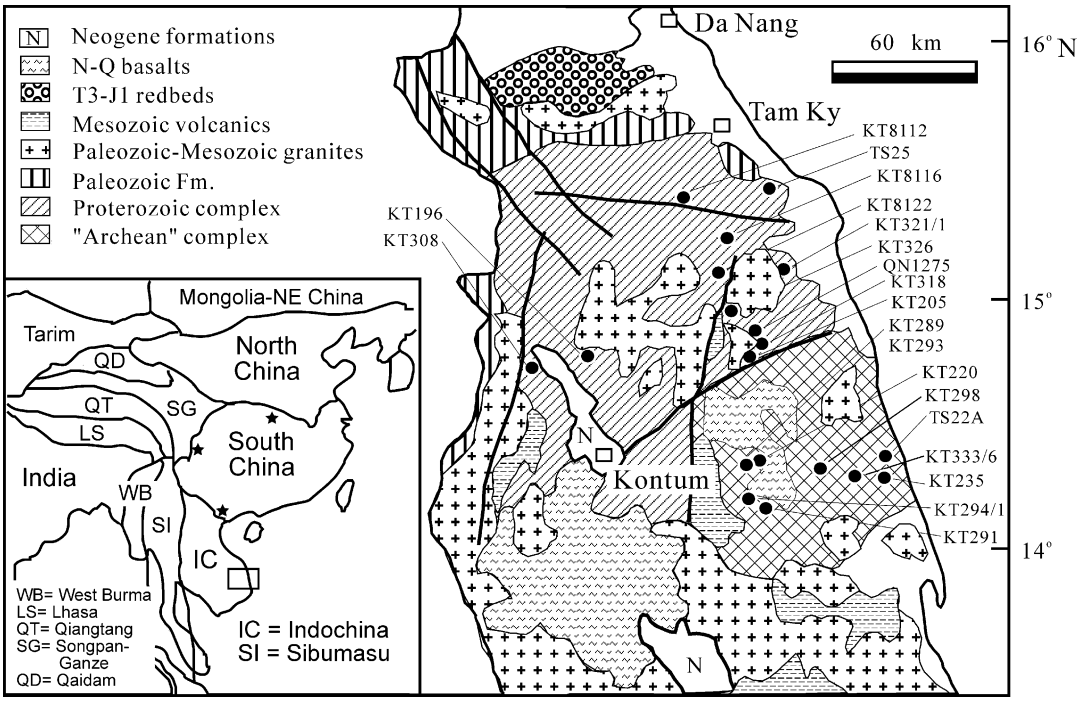

Fig. 1. Simplified geological map of the northern Kontum massif, central Vietnam (modified from Nam, 1998) showing the basement rocks and sample localities of this study. Samples KT8049/1 and KT8049 are located further south at 13°21.8′N and are not shown in the map. "Archean" complex is composed mainly of Kannack and Song Ba complexes while other formations and complexes belong to Proterozoic complex. Inset map showing the distribution of principal continental terranes of East and Southeast Asia (Metcalfe, 1998) and the location of the simplified geological map. Stars denote the locations of the Archean rocks in the South China block.

Asian continent during Paleozoic to Mesozoic periods (Metcalfe, 1996, for review). The Song Ma belt, characterized by the occurrence of metamorphic mafic and ultramafic masses of ophiolitic fragments, represents the plate boundary between Indochina and South China blocks. The suturing may have taken place in the early Triassic and caused the early phase of Indosinian orogeny (Lepvrier et al., 1997; Chung et al., 1999), although the fossil fish record favors a close geographic association of the two blocks during Devonian time (Thanh et al., 1996). Thus, Vietnam is composed of two continental blocks. The part north of the Song Ma suture belongs to South China block and the part south of the suture belongs to Indochina block.

Amphibolite and granulite facies metamorphic rocks of the Kontum massif in central Vietnam have been traditionally regarded as an exposed "Archean" core complex of the Indochina block (Hutchison, 1989; Tien, 1991; Bao et al., 1994). However, the inferred "Archean" ages were basically based on the petrological correlations that link the Kontum massif with the classic Archean granulites terranes in Gondwanaland, such as those in East Antarctica, India, Sri Lanka and Australia (Katz, 1993). Without any analytical details, a Pb isochron age of 2300 Ma and K–Ar age of 1650–1810 Ma were given for the Kontum massif by Hutchison (1989). Recently, radiometric ages have been reported for the metamorphic rocks from the Kontum massif using various methods including K–Ar (Nam, 1998), $^{40}Ar/^{39}Ar$ (Lo et al., 1999), SHRIMP U–Pb zircon (Carter et al., 2001; Nam et al., 2001), composite $^{40}Ar/^{39}Ar$ and U–Pb (Nagy et al., 2001) techniques. The results show Permo-Triassic ages (~250 Ma) for 10 samples and mid- to late-Paleozoic ages (~450 Ma) for four samples. The presumed Precambrian age of Kontum massif has been obtained in a zoned zircon

core from a gneiss yielding a concordant age of 1403 ± 34 Ma (Nam et al., 2001), in addition to some upper intercept ages for zircons from 1.1 to 2.7 Ga (Nagy et al., 2001). Geochronological studies have also been performed for rocks north of the Kontum massif and south of the Song Ma suture using $^{40}Ar/^{39}Ar$ (Lepvrier et al., 1997; Jolivet et al., 1999), K–Ar (Nam, 1998), composite Rb–Sr and U–Pb (Nagy et al., 2000) and SHRIMP U–Pb zircon (Carter et al., 2001) methods. The results yielded a wide age range including Oligocene-Miocene (19.6 ± 0.5 to 36.1 ± 1 Ma), Cretaceous (82 ± 10 to 130 ± 3 Ma), Permo-Triassic (∼250 Ma), mid- to late-Paleozoic (∼450 Ma) and Neoproterozoic (800 to 901 ± 26 Ma). Precambrian ages were registered in inherited zircon cores ranging from 800 to 2541 ± 69 Ma (Carter et al., 2001) and upper intercept discordant zircons ages of 881 ± 26 to 901 ± 26 Ma (Nagy et al., 2000). The interpretation of these ages will be discussed in latter sections.

High-grade metamorphic rocks have resided at deep crustal levels for substantial periods of time. Thus, high-grade terrains provide important clues to the composition, tectonic setting and evolution of the lower continental crust. However, the high-grade metamorphic rocks of central Vietnam have been rarely subjected to detailed geochemical and isotopic studies. This paper presents the first systematic study of major and trace element as well as Sr and Nd isotopic compositions for amphibolite to granulite facies metamorphic basement rocks from the Kontum massif in order to constrain the crustal evolution of the Indosinian block.

2. Geological background

In the Indochina block, the Kontum massif represents the largest continuous exposure of Precambrian basement rocks and has been viewed as a "stable" exposure of high-grade metamorphic rocks. They can be divided into an "Archean" complex and a Proterozoic complex (Fig. 1), which are further grouped into different units under local names (Bao et al., 1994). These are metamorphic units of the Kannack complex, the Tak Po formation and the Kham Duc formation and magmatic complexes including the Song Ba, Song Re and Chu Lai complexes (Table 1).

The Kannack complex, distributed in the central part of Kontum massif, is the major constituent of the "Archean" complex. It is composed mainly of two-pyroxene-bearing granulites, in association with plutons of orthopyroxene-bearing granite (charnockite and enderbite) and cordierite-sillimanite-bearing gneisses (khondalites). Mineral assemblages of the Kannack complex are typical of granulite facies metamorphism, with the peak *T–P* conditions of 800–850 °C and 8 ± 1 kbar (Department of Geology and Minerals of Vietnam—DGMVN, 1989). Proterozoic formations are widely distributed in the Kontum massif and are composed of gneiss, amphibolite, schist, migmatite and lenses of marble. Mineral assemblages of these Proterozoic rocks suggest an amphibolite facies metamorphism (DGMVN, 1989).

The Kannack complex and the intrusive Song Ba complex were speculated to be "Archean" (>2.6 Ga, Tien, 1991; Bao et al., 1994) based solely on their petrological similarities with the Archean granulites in other parts of the world. However, the recent geochronological studies for gneisses, migmatites and charnockites (Nam, 1998; Nam et al., 2001; Carter et al., 2001; Nagy et al., 2001) from such an "Archean" Kannack complex showed Permo-Triassic ages (240.6 ± 5.0 to 258±6 Ma). Moreover, both Permo-Triassic and mid- to late-Paleozoic ages (407 ± 11 to 451 ± 3 Ma) were obtained for the gneiss, granodiorite and amphibolite samples from the surrounding Proterozoic complex (Carter et al., 2001; Nagy et al., 2001). SHRIMP U–Pb ages (Chung et al., unpublished data) were obtained on zircons in two of the samples in this study (KT289, a charnockite from the "Archean" Song Ba complex, and KT318, a gneiss from the Proterozoic Song Re complex). Zircons from KT289 give a concordant age of 260 ± 16 Ma. The majority of zircons from KT318 give concordant ages of 436 ± 10 Ma but three zircons give ages of 2541 ± 55, 1455 ± 24 and 869 ± 57 Ma, which we interpreted to be inherited ages. The Paleozoic age registered in the Proterozoic complex has been interpreted as indicative of a rifting event (Hutchison, 1989; Carter et al., 2001; Nagy et al., 2001) that disintegrated the Indochina block from Gondwanaland. The Indosinian age registered in both the "Archean" and Proterozoic complexes has been widely considered to record the granulite facies to amphibolite facies metamorphism (Lepvrier et al., 1997; Nam et al., 2001; Carter et al., 2001).

Table 1
Major and trace element concentration for basement rocks from central Vietnam

Sample no.	KT321/1E	KT321/1	KT326	QN1275	KT318	KT308	KT196	KT205
Latitute	15°7.3′	15°7.3′	15°0′	14°50′	14°46.5′	14°43′	14°46′	14°45′
Longitude	108°36.9′	108°36.9′	108°30.5′	108°32′	108°31.7′	107°43′	107°53.5′	108°31.5′
Complex	Tu Mo Rong	Tu Mo Rong	Tu Mo Rong	Song Re	Song Re	Tak Po	Tak Po	Kham Duc
Rock type[a]	Mafic Gneiss	Mgm Gneiss	Mgm Gneiss	Bt Gneiss	Bt Gneiss	Bt Gneiss	Bt Gneiss	Bt Gneiss
Major element (%) by XRF								
SiO_2	53.32	63.00	71.82	63.45	68.65	62.32	71.71	64.29
TiO_2	0.37	0.42	0.23	0.92	0.40	0.83	0.29	0.76
Al_2O_3	11.46	13.90	15.27	15.63	15.04	17.64	14.49	14.87
Fe_2O_3	1.69	1.02	0.47	1.30	0.79	0.83	0.14	1.50
FeO	7.63	4.30	1.62	3.91	2.65	4.24	2.57	4.39
MnO	0.24	0.11	0.07	0.08	0.08	0.07	0.06	0.10
MgO	11.07	5.61	0.59	1.77	1.04	1.76	0.66	2.23
CaO	9.71	5.62	3.24	4.42	3.23	5.02	2.09	4.77
Na_2O	1.07	1.41	3.95	2.56	2.63	4.02	2.71	2.14
K_2O	1.47	2.58	1.99	4.08	4.49	2.07	3.91	2.47
P_2O_5	0.08	0.15	0.13	0.40	0.16	0.22	0.08	0.13
LOI	2.00	1.73	0.76	1.24	0.76	1.05	0.81	1.90
Total	100.11	99.85	100.14	99.76	99.92	100.07	99.52	99.55
Trace element (ppm) by XRF + ICP-AES								
Rb	125.0	233.0	96.4	121.9	155.3	89.9	141.2	104.9
Ba	139	259	313	1319	718	495	492	865
Sr	142	252	136	254	210	319	134	307
Zr	53	122	189	366	241	382	150	151
Y	28.6	19.3	21.9	34.6	42.3	28.2	35.3	28.2
Cr	1101	349	11	28	21	21	23	36
V	203	132	24	112	64	67	39	133
Sc	35	25	7	18	14	15	9.3	20.5
Ni	226	71	<0.5	12	4	6	4	11
Co	35	17	3	10	7	10	5	12
Cu	5	5	4	16	7	9	7	15
Zn	94	57	36	67	49	60	41	78
Ga	10.8	9.7	9.2	12.1	10.4	18.7	15.2	15.6
Trace element (ppm) by ICP-MS								
La	11.6	30.8	34.5	43.7	38.0	55.4	32.7	53.1
Ce	25.5	59.8	62.7	89.5	76.0	106.8	66.1	97.5
Pr	3.0	6.9	6.9	11.0	8.1	10.6	8.0	11.3
Nd	12.1	26.6	24.4	42.2	30.2	39.3	29.4	40.5
Sm	3.0	4.7	4.7	8.3	6.2	6.7	5.8	7.7
Eu	0.79	0.85	0.82	2.22	1.00	1.30	1.12	1.68
Gd	2.92	4.49	4.64	8.17	5.42	5.05	5.79	6.72
Tb	0.55	0.66	0.79	1.16	0.97	0.77	0.98	1.08
Dy	3.63	3.78	4.87	6.39	5.70	4.38	5.93	6.19
Ho	0.75	0.78	1.06	1.27	1.14	0.80	1.24	1.21
Er	2.04	2.19	2.96	3.25	3.20	2.03	3.67	3.35
Tm	0.32	0.35	0.46	0.44	0.53	0.31	0.58	0.47
Yb	2.13	2.20	3.12	2.58	3.31	1.80	3.75	2.91
Lu	0.32	0.34	0.50	0.38	0.49	0.27	0.56	0.43
Th	3.61	12.23	16.54	10.97	27.68	16.14	12.27	14.03
U	1.00	2.49	3.27	2.01	4.41	0.92	1.39	2.05
Hf	1.5	3.9	5.6	8.6	6.1	7.5	3.8	5.7
Nb	4.6	4.0	7.5	17.8	12.1	14.9	7.9	12.9
Ta	0.36	0.50	0.65	0.88	0.81	0.33	0.42	0.91
Y	26	21	29	33	36	26	36	33
Cr	1140	325	16	31	30	26	42	61
V	197	130	21	109	60	69	32	118
Ni	281	75	46	13	9	11	8	
Co	42	23	4	13	8	11	4	15

Table 1 (*Continued*)

Sample no.	KT294/1	KT333/6	KT220	KT8049/1	KT8049	KT8122	TS25
Latitute	14°12′	14°14′	14°16′	13°21.8′	13°21.8′	15°5′	15°26.72′
Longitude	108°32′	108°54.9′	108°32.5′	108°25′	108°25′	108°24.6′	108°35.24′
Complex	Kannack	Song Ba	Kham Duc	Song Re	Song Re	Tak Po	Dieng Bong
Rock type[a]	Gt Cd Gneiss	Mgm Gneiss	Bt Gneiss	Felsic Gneiss	Am Schist	Bt Schist	Am Schist
Major element (%) by XRF							
SiO_2	58.36	61.94	71.67	72.14	57.41	59.92	61.83
TiO_2	1.62	0.60	0.30	0.17	0.76	1.01	0.49
Al_2O_3	18.49	20.94	14.37	15.16	13.65	17.93	18.08
Fe_2O_3	0.63	1.07	0.72	0.26	1.21	2.57	2.08
FeO	6.06	1.57	1.38	1.52	7.29	4.19	2.53
MnO	0.07	0.04	0.02	0.03	0.20	0.09	0.07
MgO	2.41	1.01	0.51	0.54	6.09	2.18	2.56
CaO	6.28	1.42	2.38	2.80	7.70	6.05	5.16
Na_2O	2.42	4.37	2.14	4.04	1.73	1.92	4.67
K_2O	1.42	4.47	5.08	2.20	1.35	2.23	1.24
P_2O_5	0.62	0.08	0.08	0.06	0.10	0.42	0.21
LOI	1.42	2.08	0.64	1.43	2.59	1.68	1.12
Total	99.80	99.59	99.29	100.35	100.08	100.19	100.04
Trace element (ppm) by XRF + ICP-AES							
Rb	93.3	116.6	150.2	121.8	78.0	86.7	34.9
Ba	593	1183	1420	378	261	462	473
Sr	244	237	212	279	114	719	848
Zr	655	306	192	106	134	137	83
Y	17	9.9	14.8	11.8	33	13.8	10.6
Cr	5	101	15	8	301	7	51
V	116	59	32	14	227	81	118
Sc	12	3	7.6	5	36	10	10
Ni	3	11	3	<0.5	61	5	18
Co	10	5	2	4	30	13	13
Cu	14	21	8	9	23	60	5
Zn	119	47	31	29	100	93	64
Ga	23.5	18.4	12.8	11.2	12.7	16.5	20.9
Trace element (ppm) by ICP-MS							
La	45.7	72.1	58.4	21.0	25.4	36.9	19.1
Ce	106.6	118.8	101.9	38.6	49.6	78.8	39.4
Pr	13.5	13.0	11.1	3.9	6.3	10.6	4.9
Nd	53.6	44.7	37.6	13.0	24.1	42.6	17.6
Sm	9.8	6.4	5.5	2.1	5.1	8.5	2.9
Eu	1.63	2.52	1.74	0.59	0.99	2.17	0.91
Gd	7.70	5.06	4.22	1.63	5.14	7.19	2.61
Tb	0.89	0.58	0.61	0.26	0.89	0.97	0.37
Dy	3.74	2.23	3.22	1.52	5.82	4.61	2.09
Ho	0.64	0.38	0.60	0.31	1.23	0.77	0.40
Er	1.41	1.02	1.71	0.85	3.51	1.93	1.09
Tm	0.17	0.15	0.24	0.15	0.52	0.24	0.16
Yb	1.03	1.00	1.40	1.03	3.24	1.35	1.01
Lu	0.16	0.18	0.22	0.16	0.50	0.19	0.16
Th	6.62	28.91	15.77	7.28	12.77	5.69	4.15
U	0.95	2.98	1.57	1.18	3.64	2.55	0.85
Hf	14.9	10.1	6.7	2.4	2.1	6.1	2.5
Nb	19.9	15.6	7.6	8.4	8.9	13.5	4.4
Ta	1.11	1.50	0.60	0.55	0.88	0.85	0.39
Y	16	11	17	10	37	21	12
Cr	5	92	43	12	256	37	62
V	94	51	28		210	76	95
Ni	4	19	10	10	63	7	22
Co	11	6	4	3	36	16	12

Table 1 (*Continued*)

Sample no.	KT298	TS22A	KT235	KT8112	KT8116	KT291	KT289	KT293
Latitude	14°15.2′	14°22.31′	14°19′	15°23′	15°13′	14°10.36′	14°15.7′	14°14.3′
Longitude	108°45.2′	109°6.42′	109°3′	108°16′	108°25.6′	108°34.37′	108°30.2′	108°30.6′
Complex	Kannack	Phu My	Phu My	Kham Duc	Kham Duc	Song Ba	Song Ba	Kannack
Rock type[a]	Amphibolite	Amphibolite	Amphibolite	Amphibolite	Amphibolite	Charnockite	Charnockite	Granulite
Major element (%) by XRF								
SiO_2	48.22	45.44	50.22	49.23	54.36	45.33	57.61	49.46
TiO_2	1.60	1.85	1.07	2.00	0.49	1.85	1.05	1.12
Al_2O_3	12.93	15.37	14.74	13.81	13.11	20.47	17.81	15.39
Fe_2O_3	1.86	4.10	1.82	2.49	2.16	0.75	1.66	0.41
FeO	8.94	13.46	10.87	10.36	10.90	9.88	5.18	11.06
MnO	0.34	0.21	0.21	0.22	0.20	0.18	0.12	0.20
MgO	8.82	5.64	6.46	6.05	5.64	4.50	3.45	7.54
CaO	10.85	9.68	9.70	10.06	9.36	11.32	6.60	12.64
Na_2O	0.36	2.42	1.56	3.51	2.02	1.53	3.81	0.82
K_2O	2.14	0.21	0.88	0.31	0.29	1.24	1.16	0.24
P_2O_5	0.16	0.05	0.07	0.22	0.06	0.70	0.47	0.10
LOI	3.25	1.79	1.92	1.80	1.89	1.83	1.09	0.99
Total	99.47	100.22	99.52	100.06	100.48	99.58	100.01	99.97
Trace element (ppm) by XRF + ICP-AES								
Rb	105.8	6.4	23.0	9.9	8.4	62.7	20.5	11.5
Ba	196	23	144	36	27	434	180	32
Sr	120	200	96	134	50	435	473	115
Zr	95	38	59	143	23	412	191	47
Y	33.9	11.1	24.5	42.6	18.8	68	18.4	23.0
Cr	328	29	133	156	90	6	55	133
V	308	779	387	368	317	173	140	324
Sc	48	32	43.9	44	52	37	15	43
Ni	55	12	84	50	57	4	17	75
Co	36	88	44	39	45	21	15	44
Cu	155	359	127	71	45	20	18	37
Zn	120	105	103	113	101	124	98	101
Ga	13.0	22.6	15.3	15.3	9.1	22.1	19.6	14.0
Trace element (ppm) by ICP-MS								
La	8.9	1.5	6.0	7.1	0.7	33.7	30.1	8.7
Ce	24.5	9.3	17.4	18.3	1.9	93.6	69.0	22.0
Pr	3.8	1.5	2.7	3.1	0.3	13.7	8.7	3.2
Nd	17.6	6.2	10.5	15.2	1.9	61.4	35.7	14.3
Sm	4.7	1.8	2.6	4.7	0.8	13.0	6.5	3.6
Eu	2.20	0.67	0.94	1.60	0.36	2.31	1.28	0.88
Gd	5.36	1.87	3.62	6.04	1.59	12.30	5.26	3.93
Tb	0.93	0.32	0.63	1.05	0.34	1.96	0.69	0.63
Dy	6.25	2.04	4.14	7.41	2.72	11.85	3.52	3.96
Ho	1.28	0.44	0.87	1.57	0.65	2.39	0.61	0.80
Er	3.62	1.18	2.55	4.43	2.03	6.57	1.48	2.11
Tm	0.53	0.19	0.39	0.64	0.32	0.98	0.21	0.33
Yb	3.39	1.18	2.44	4.04	2.14	6.56	1.30	2.11
Lu	0.51	0.18	0.38	0.62	0.35	0.96	0.17	0.31
Th	0.95	0.24	1.37	0.61	0.06	1.48	0.41	0.57
U	0.84	0.18	0.59	0.20	0.02	0.59	0.24	0.11
Hf	1.03	0.98	1.83	1.26	0.46	10.2	4.5	1.7
Nb	12.12	1.38	3.58	5.77	0.82	20.9	9.3	6.0
Ta	0.73	0.18	0.35	0.37	0.06	0.89	0.44	0.44
Y	37	12	24	46	18	65	18	21
Cr	289	33	152	136	71	6	60	144
V	295	708	358	359	308	158	124	301
Ni	71	12	95	54	66	6		100
Co	47	74	50	47	56	23	19	49

[a] Am: amphibole; Bt: biotite; Cd: cordierite; Gt: garnet; Mgm: migmatite.

3. Samples and petrography

Samples of the Kontum massif were collected from the "Archean" and Proterozoic complexes (Fig. 1). They include different rock types (gneiss and schist, amphibolite, charnockite and granulite) from different formations and plutons (Table 1). The gneisses are composed of quartz, K-feldspar, plagioclase, ±muscovite, ±brown biotite, ±greenish-brown amphibole, opaque, ±apatite, ±epidote, ±chlorite, and ±garnet. The schists consist of quartz, feldspar, ±brown biotite, ±greenish-brown amphibole, epidote, and opaque. The amphibolites contain plagioclase, greenish-brown amphibole, ±brown biotite, ±garnet and minor opaque, sphene, ±epidote, ±chlorite. Both charnockite and granulite consist of pale pink to green pleochroic orthopyroxene, clinopyroxene, plagioclase, ±brown biotite, ±greenish brown amphibole and minor opaque (ilmenite, pyrite), apatite, ±epidote.

4. Analytical techniques

4.1. Whole rock chemistry

Major and 11 trace element (Rb, Ba, Sr, Zr, Y, Cr, V, Ni, Cu, Zn and Ga) concentrations were determined in the Department of Geosciences, Franklin and Marshall College, USA, using X-ray fluorescence (XRF) techniques on fused glass disks and pressed powder briquettes, respectively. Working curves were constructed using at least 50 analyzed geochemical rock standards (Abbey, 1983; Govindaraju, 1994). The amount of ferrous Fe was titrated using a modified Reichen and Fahey (1962) method, and loss on ignition was determined by heating an exact aliquot of the sample at 950 °C for 1 h. Concentrations of two of the trace elements (Sc and Co) were determined using ICP-AES spectrometer, also at Franklin and Marshall College. Analytical uncertainties range from 1 to 5% for major elements and from 2 to 10% for minor elements. Details of the analytical procedures can be found in Boyd and Mertzman (1987) and Mertzman (2000).

The concentrations of 14 rare earth elements (REE) and 10 trace element (Th, U, Hf, Nb, Ta, Y, Cr, V, Ni and Co) concentrations were analyzed at the Guangzhou Institute of Geochemistry, Chinese Academy of Sciences, Guangzhou, using a Perkin-Elmer Sciex ELAN 6000 inductively-coupled plasma mass spectrometer (ICP-MS). The analytical procedures and accuracy were reported in Li (1997). The uncertainties for all elements are less than 5%.

4.2. Sr and Nd isotopic data

Samples were analyzed for Sr and Nd isotopic composition as well as Sm and Nd concentrations using a VG354 mass spectrometer for Sr and MAT262 for Sm and Nd at the Institute of Earth Sciences, Academia Sinica, Taipei. Sr, Sm and Nd separation was achieved using conventional cation-exchange chromatography (Lan et al., 1986; Shen et al., 1993). Sr was loaded on a single Ta filament while Sm and Nd were loaded on a single Re filament and analyzed as mono-oxide ions. The isotopic compositions were measured in multi-collectors with dynamic mode. The isotopic ratios were corrected for mass fractionation by normalizing to $^{86}Sr/^{88}Sr = 0.1194$ and $^{146}Nd/^{144}Nd = 0.7219$, respectively. Values for the NBS987 Sr standard yielded $^{87}Sr/^{86}Sr = 0.710240$ with a long-term reproducibility of 0.000028 (95% confidence level) and for the La Jolla (UCSD) Nd standard, yielded $^{143}Nd/^{144}Nd = 0.511866$ with a long-term reproducibility of 0.000026.

5. Results

Major and trace element concentrations of the analyzed samples are presented in Table 1 and their isotopic data are presented in Table 2. It should be noted that all the rocks have experienced high-grade regional metamorphism and recrystallization. K, Na and low-field-strength elements (LFSE: Rb, Sr, Ba) were likely mobilized during amphibolite facies metamorphism (e.g. Humphris and Thompson, 1978). Thus, these elements are not used for the petrogenetic interpretations. Diagrams of Zr/TiO_2 versus Nb/Y of Winchester and Floyd (1977) and FeO^*/MgO versus SiO_2 of Miyashiro (1974) are applied in Fig. 2 for the classification and distinction of calc-alkaline from tholeiitic for the basement rocks. Sm–Nd model ages (depleted mantle (DM) model age $-T_{DM}$) or crustal residence ages are calculated assuming a linear evolution of DM from $\varepsilon_{Nd} = 0$ at 4.56 Ga to $\varepsilon_{Nd} = +10$

Table 2
Sr and Sm–Nd isotopic compositions for basement rocks from central Vietnam

Sample no.	$^{87}Sr/^{86}Sr$[a]	$\pm 2\sigma$	Sm[b] (ppm)	Nd[b] (ppm)	$^{147}Sm/^{144}Nd$	$^{143}Nd/^{144}Nd$[c]	$\pm 2\sigma$	$\varepsilon_{Nd}(0)$[d]	$\varepsilon_{Nd}(T)$[e]	T_{DM}[f] (Ga)
Gneiss										
KT321/1E	0.72035	1	4.73[b]	26.60[b]	0.1075	0.512213	12	−8.3	−3.2	1.3
KT321/1	0.72112	1	4.43	24.02	0.1115	0.512025	10	−12.0	−7.1	1.7
KT326	0.71966	1	5.50	28.74	0.1157	0.512233	12	−7.9	−3.3	1.4
QN1275	0.72257	2	9.34	45.14	0.1251	0.512020	13	−12.1	−8.0	1.9[g]
KT318	0.72592	2	8.01	36.97	0.1310	0.511975	12	−12.9	−9.2	2.2[g]
KT308	0.71491	1	6.69[b]	39.34[b]	0.1028	0.512189	13	−8.8	−3.4	1.3
KT196	0.79198	2	7.36	34.19	0.1302	0.511978	5	−12.9	−9.1	2.1
KT205	0.71742	2	7.09	38.56	0.1112	0.511919	6	−14.0	−9.1	1.8
KT294/1	0.74511	2	11.63	59.78	0.1176	0.511858	11	−15.2	−12.7	2.0[g]
KT333/6	0.78673	2	6.50	44.71	0.0879	0.511521	13	−21.8	−18.3	2.0[g]
KT220	0.72583	2	5.57	37.72	0.0893	0.511865	11	−15.1	−11.7	1.6
KT8049/1	0.73706	2	2.10[b]	12.96[b]	0.0980	0.511817	15	−16.0	−10.4	1.8[g]
Schist										
KT8049	0.75360	2	5.11[b]	24.05[b]	0.1285	0.511832	12	−15.7	−11.8	2.4[g]
KT8122	0.70892	1	8.52[b]	42.64[b]	0.1208	0.512397	14	−4.7	−0.3	1.2
TS25	0.70621	1	2.89	15.73	0.1111	0.512323	19	−6.1	−1.2	1.2
Amphibolite										
KT298	0.76486	1	4.67[b]	17.60[b]	0.1604	0.512610	15	−0.6	+1.5	
TS22A	0.70589	2	1.34	4.51	0.1796	0.512675	16	+0.7	+1.7	
KT235	0.71839	2	2.61[b]	10.46[b]	0.1509	0.512478	15	−3.1	−0.5	
KT8112	0.70636	1	4.99	15.80	0.1910	0.512910	14	+5.3	+5.6	
KT8116	0.70889	1	0.93	2.04	0.2756	0.513397	12	+14.8	+10.3	
Charnockite										
KT291	0.71595	1	13.04[b]	61.38[b]	0.1285	0.512062	16	−11.2	−9.1	1.9[g]
KT289	0.71069	1	6.54[b]	35.68[b]	0.1108	0.512136	16	−9.8	−7.1	1.5[g]
Granulite										
KT293	0.72209	2	3.75	14.51	0.1563	0.512128	14	−10.0	−8.7	2.7[g]

[a] Our long-term measured ratio for the NBS987 Sr standard being 0.710240 ± 0.000028.
[b] Concentration obtained by ICP-MS method, error ±5%; others obtained by ID method using TIMS, uncertainty ±0.5%.
[c] Our long-term measured ratio for the La Jolla Nd standard being 0.511866 ± 0.000026.
[d] $\varepsilon_{Nd}(0) = [(^{143}Nd/^{144}Nd)_{sample}/0.512638 - 1] \times 10^4$.
[e] $\varepsilon_{Nd}(T) = [(^{143}Nd/^{144}Nd)_{sample}(T)/(^{143}Nd/^{144}Nd)_{CHUR}(T) - 1] \times 10^4$, $(^{143}Nd/^{144}Nd)_{sample}(T) = (^{143}Nd/^{144}Nd)_{sample} - (^{147}Sm/^{144}Nd)_{sample}$ $(\exp \lambda T - 1)$, $(^{143}Nd/^{144}Nd)_{CHUR}(T) = 0.512638–0.1967\ (\exp \lambda T - 1)$, $\lambda = 0.00654\,Ga^{-1}$, $T = 250$ Ma for gneiss: KT294/1, KT333/6, KT220, charnockite and granulite; $T = 450$ Ma for others.
[f] Crustal residence model age assuming derivation from a depleted mantle source with present ε_{Nd} of +10, $T_{DM} = 1/\lambda \times \ln\{1 + [(^{143}Nd/^{144}Nd)_{sample} - 0.51315]/[(^{147}Sm/^{144}Nd)_{sample} - 0.2137]\}$.
[g] Model ages represented the first crust-forming stage, others represented the second stage.

at the present time (Goldstein et al., 1984). We have limited samples with $^{147}Sm/^{144}Nd$ close to the average crustal value and less than 0.16, such that meaningful Sm–Nd model ages can be obtained to trace the crustal evolutionary history. Most amphibolites have $^{147}Sm/^{144}Nd$ higher than 0.16, so that their model ages are geologically meaningless. The chondrite values used for REE normalization are from Masuda et al. (1973) divided by 1.2 and the primitive mantle values used for spidergram construction are from Sun and McDonough (1989).

5.1. Geochemical characteristics of the basement rocks

5.1.1. Gneiss and schist

The gneisses have a wide range in SiO_2 (58.3–72.1%). They all show high Al_2O_3 (13.9–20.9%) and

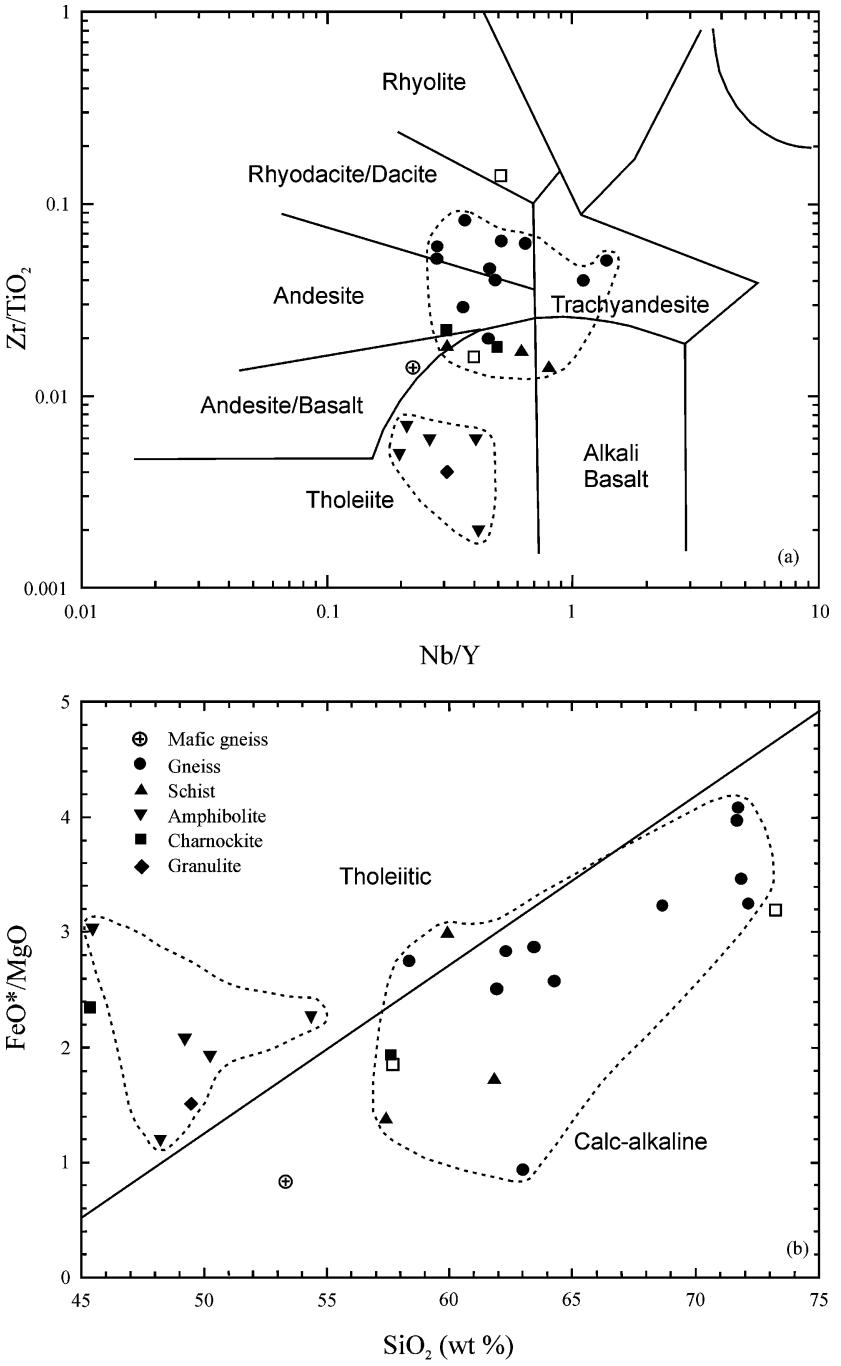

Fig. 2. (a) Zr/TiO_2 vs. Nb/Y diagram of Winchester and Floyd (1977) for the classification of different rock types and (b) FeO^*/MgO vs. SiO_2 diagram of Miyashiro (1974) for the distinction of calc-alkaline from tholeiitic rocks for basement rocks from the Kontum massif, central Vietnam. Two charnockites of Nagy et al. (2001) are shown by open squares.

high ASI (aluminum saturation index = molecular proportion of $Al_2O_3/(CaO + Na_2O + K_2O)$, 0.9–1.2 mostly) except for the enclave (a mafic gneiss KT321/1E) which possesses lower SiO_2 (53.3%) and Al_2O_3 (11.5%). The schists have intermediate compositions with SiO_2 ranging from 57.4 to 61.8%. In Fig. 2a, it can be seen that most gneisses belong to the rhyodacite/dacite and trachyandesite fields while schists possess low Zr/TiO_2 and belong to the andesite/basalt to alkali basalt fields. Both gneisses and schists plot in the calc-alkaline field (Fig. 2b) except for gneiss KT294/1 and schist TS25.

The REE distribution patterns for the gneisses and schists can be divided into two groups. The first group is represented by the samples of eight gneisses (Fig. 3a), two schists (KT8122, TS25) from the Proterozoic complex north of the "Archean" complex, and one gneiss (KT8049/1) and one schist (KT8049) from the Proterozoic complex south of the "Archean" complex (Fig. 3b). This group shows moderately fractionated REE patterns ($5.7 \leqq (La/Yb)_N \leqq 20.3$, except KT321/1E of 3.6) with low light REE (LREE) ($60 \leqq La_N \leqq 176$, except KT321/1E of 36.7), high heavy REE (HREE) ($8.6 \leqq Yb_N \leqq 18$, except KT8049/1 and TS25 of 4.9 and KT8122 of 6.5) and marked negative Eu anomalies ($Eu/Eu^* = 0.5$–0.8, except KT8049/1 and TS25 of 0.9). Such characteristics are often observed in crust-derived, anatectic peraluminous granites (Rogers and Greenberg, 1990; Holtz and Barrey, 1991) as well as in post-Archean sediments (Haskin et al., 1966; André et al., 1986). The second group is represented by three gneisses (KT294/1, KT333/6 and KT220) from the "Archean" complex (Fig. 3b). They show strongly fractionated ($27.5 \leqq (La/Yb)_N \leqq 47.6$) REE patterns with high LREE ($145 \leqq La_N \leqq 229$) and low HREE ($4.8 \leqq Yb_N \leqq 6.7$) contents and positive Eu anomalies ($1.0 \leqq Eu/Eu^* \leqq 1.3$, except KT294/1 of 0.6). The strongly fractionated REE patterns, low Yb contents and no significant Eu anomalies for these gneisses are similar to those of Archean tonalite-trondhjemite-granodiorite (TTG) (usually $(La/Yb)_N > 20$, $0.3 \leqq Yb_N \leqq 8.5$; Martin, 1994). In the spidergrams (Fig. 4a and b), both groups display similar Nb, Ta, (Sr), P and (Ti) negative anomalies, but the second group differs in having lower Y and HREEs. In addition, the mafic gneiss (KT321/1E) contains the highest Cr and Ni and lowest $(La/Yb)_N$ ratio (3.6) among all the analyzed samples. The migmatitic gneiss (KT333/6) having the lowest $\varepsilon_{Nd}(0)$ contains low Fe and Mg, and the highest Al_2O_3 (20.9%), ASI (1.4) and LREE contents.

In Fig. 5a and b, all the gneisses and schists are plotted in $(La/Yb)_N$ versus Yb_N and (Sr/Y) versus Y spaces. Five gneisses (four gneisses of Figs. 3b and 4b plus KT308) and two schists (except KT8049 in Figs. 3b and 4b) lie in the field of Archean TTG and modern adakite of Martin (1986) (Fig. 5a), but most samples fall in the overlap field between Archean and post-Archean rocks. Two gneisses (KT333/6 and KT8049/1 in Figs. 3b and 4b) and one schist (TS25 in Figs. 3b and 4b) plot in the field of Archean TTG and modern adakite of Drummond and Defant (1990) (Fig. 5b). The remaining gneisses and schists lie in classical calc-alkaline island arc field. Thus, the geochemical characteristics of most analyzed gneisses and schists from the Kontum massif are similar to those of post-Archean granitoid and island arc material, despite a few samples which reveal geochemical similarities with Archean TTGs. All of our rocks show depletions in the high field strength elements (HFSE; e.g. Nb, Ta and Ti) and can be interpreted as derived from pre-existing crustal materials.

5.1.2. Amphibolites

The five amphibolites have low SiO_2 (45.4–54.4%) and variable mg-values (atomic $100Mg/(Mg + Fe^{2+})$) of 42–63. Although the amphibolites are tholeiitic in composition (Fig. 2a and b), they can be separated into two types based on their TiO_2, CaO and trace element contents. The first type has 1.07–2.00% TiO_2, 9.68–10.85% CaO, 96–200 ppm Sr, 38–143 ppm Zr, 0.98–1.83 ppm Hf, 1.38–12.12 ppm Nb, 0.18–0.73 ppm Ta, 71–359 ppm Cu, 103–120 ppm Zn, 13.0–22.6 ppm Ga (Table 1) and moderately LREE-enriched patterns (Fig. 3c). They all show convex chondrite-normalized patterns in the LREE. Both positive ($Eu/Eu^* = 1.1$–1.4) and subtle negative ($Eu/Eu^* = 0.93$–0.96) Eu anomalies are observed. The second type is represented by sample KT8116 only and is characterized by lower TiO_2 (0.49%), CaO (9.36%), Sr (50 ppm), Zr (23), Hf (0.46), Nb (0.82), Ta (0.06), Cu (45), Zn (101) and Ga (9.1) contents and a strong depletion in LREE without negative Eu anomaly (Fig. 3c). Such differences indicate that the basaltic protoliths originated from two separate sources. In the spidergrams, the amphibolites (Fig. 4c)

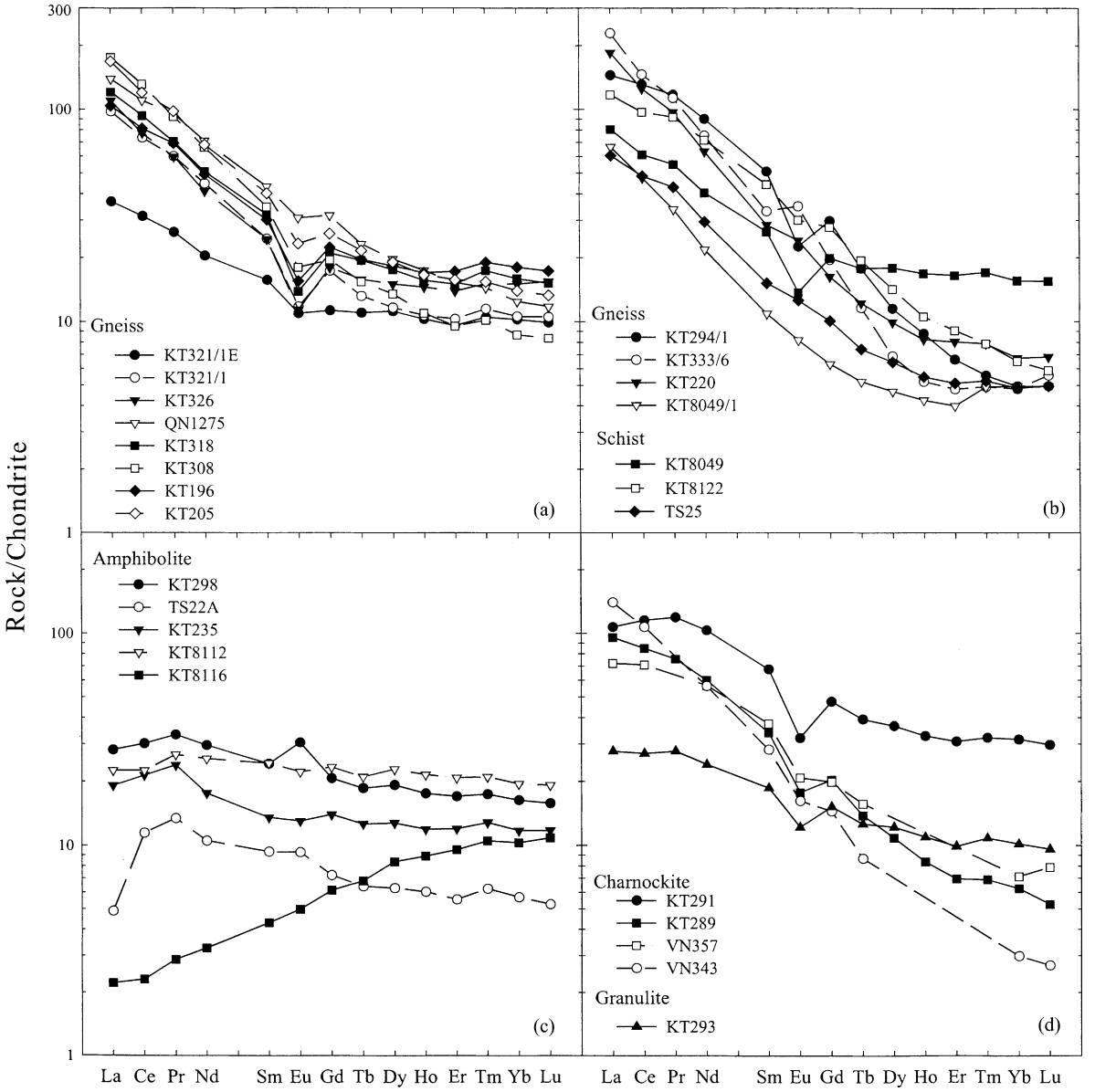

Fig. 3. Chondrite-normalized REE distribution patterns for (a) and (b) gneiss and schist, (c) amphibolite and (d) charnockite and granulite from the Kontum massif, central Vietnam. VN357 and VN343 shown as dotted lines in (d) are from Nagy et al. (2001).

lack apparent anomalies in Nb and Ta, which suggest an intraplate tectonic setting for the petrogenesis of their protoliths.

5.1.3. Charnockite and granulite

In the Zr/TiO_2 versus Nb/Y plot of Fig. 2a, the two charnockites in this study plot in the tholeiite field and not in the alkali basalt field. However, in a FeO^*/MgO versus SiO_2 plot (Fig. 2b) one sample plots in the calc-alkaline field (KT289 with 57.6% SiO_2). The two charnockites appear to be relatively evolved based on mg-values of 44 and 55 and LREE-enriched patterns (Fig. 3d) with negative Eu anomalies ($Eu/Eu^* = 0.5$ and 0.7). The calc-alkaline sample (KT289,

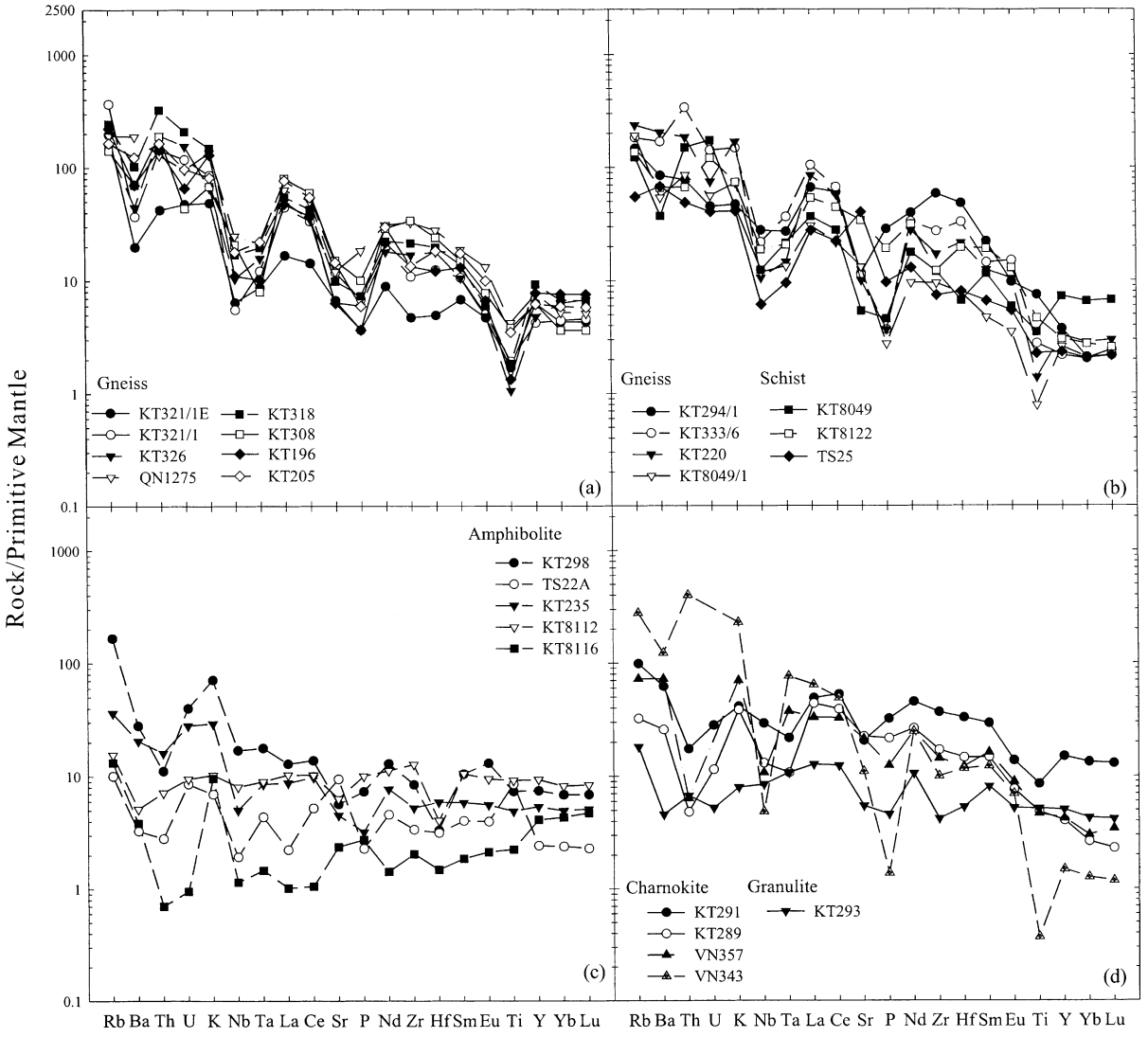

Fig. 4. Primitive mantle-normalized spidergrams for (a) and (b) gneiss and schist, (c) amphibolite and (d) charnockite and granulite from the Kontum massif, central Vietnam. VN357 and VN343 shown as dotted lines in (d) are from Nagy et al. (2001).

$(La/Yb)_N = 15.2$) displays a more fractionated REE pattern than the tholeiitic one (KT291, $(La/Yb)_N = 3.6$), although the former has lower REE abundances than the latter. In the spidergram (Fig. 4d), they have generally similar patterns, although abundances of most elements are higher for the tholeiitic one than the calc-alkaline one. They are enriched in Rb, K and LREEs, and depleted in Th, Nb and Ta. A charnockite (VN357) reported by Nagy et al. (2001) has a composition which plots in the calc-alkaline field (Fig. 2b) and shows comparable LREE enrichment (Figs. 3d and 4d) similar to KT289. Nagy et al. (2001) reported another charnockite (VN343) with significantly higher silica content (73.2%; Fig. 2b). It exhibits a higher LREE content and an apparently more fractionated REE pattern ($(La/Yb)_N = 47$) than the other charnockites (Fig. 3d). This sample shows depletions in Nb, P and Ti and strong enrichments in Th and K (Fig. 4d). The Vietnamese charnockites thus appear to be very heterogeneous.

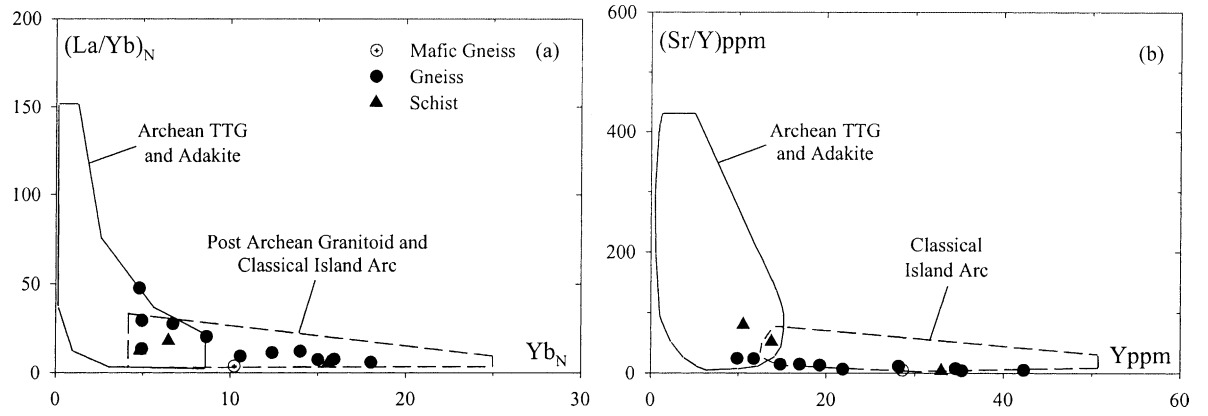

Fig. 5. (a) $(La/Yb)_N$ vs. Yb_N and (b) (Sr/Y) vs. Y diagrams of the gneisses and schists from the Kontum massif, central Vietnam. Also shown are the fields of Archean TTG and modern adakites (solid line) and post-Archean juvenile granitoids and classical calc-alkaline island arcs (dotted line) (Martin, 1986; Drummond and Defant, 1990).

The granulite sample (KT293) appears to have a tholeiitic composition (Fig. 2a and b). It also exhibits LREE-enriched pattern and negative Eu anomaly (Fig. 3d), but it has lower abundances of most trace elements and higher abundances of Cr, V, Sc, Ni, Co and Cu than those of the tholeiitic charnockites (KT291). Trace element concentrations of the granulite are similar to those of estimates of the average lower continental crust (c.f. McLennan, 2001). In the spidergram (Fig. 4d), it can be seen that the granulite is depleted in Ba, U, Sr, P and Zr, contrasting with the pattern of the tholeiitic charnockites.

5.2. Isotopic compositions of the basement rocks

The present day Nd isotopic ratios, $\varepsilon_{Nd}(0)$, of the studied samples show a wide range from +14.8 to −21.8. The gneisses and schists present a large range of negative $\varepsilon_{Nd}(0)$ from −4.7 to −21.8. A migmatitic gneiss (KT333/6), having the highest ASI, exhibits the lowest $\varepsilon_{Nd}(0)$. These rocks have crustal $^{147}Sm/^{144}Nd$ value of 0.088–0.131, whereas, the amphibolites of the first type have slightly negative to positive $\varepsilon_{Nd}(0)$ values (−3.1 to +5.3) and higher $^{147}Sm/^{144}Nd$ of 0.151 to 0.191. The amphibolite of the second type (KT8116) exhibits the highest $\varepsilon_{Nd}(0)$ value (+14.8) and $^{147}Sm/^{144}Nd$ (0.276). The charnockites and granulite show negative $\varepsilon_{Nd}(0)$ from −9.8 to −11.2 coupled with medium $^{147}Sm/^{144}Nd$ of 0.111–0.156. Overall, the analyzed basement rocks show Paleoproterozoic to Mesoproterozoic T_{DM} ages (2.4–1.2 Ga). The only exception is granulite KT293 which has a late Archean T_{DM} age (2.7 Ga). Among these basement rocks, two rock units previously believed to be Archean (the Kannack and the Song Ba complexes), in fact define a Proterozoic T_{DM} ages restricted between 2.0 and 1.5 Ga. This suggests the Kontum core complex is unlikely to be of Archean age but began its crustal evolution in the Paleoproterozoic and Mesoproterozoic. On the other hand, the present day Sr isotopic ratios of different rock types show an overlapped range from 0.7058 to 0.7920.

6. Discussion and conclusion

6.1. Proterozoic crustal formation of the Indochina block

The Sm–Nd isotopic compositions of the “Archean” and Proterozoic basement rocks and the Permo-Triassic charnockites analyzed in this study are displayed in Fig. 6. Also shown are the Oligo-Miocene granitoids from Bu Khang complex of central Vietnam (Nagy et al., 2000), Permo-Triassic (230–265 Ma) granitic plutons from the East Coast Province batholiths of Peninsular Malaysia (Liew and McCulloch, 1985), the late Archean basement rocks from the South China block (i.e. the Cavinh complex of northern Vietnam (Lan et al., 2001) and the Kongling complex

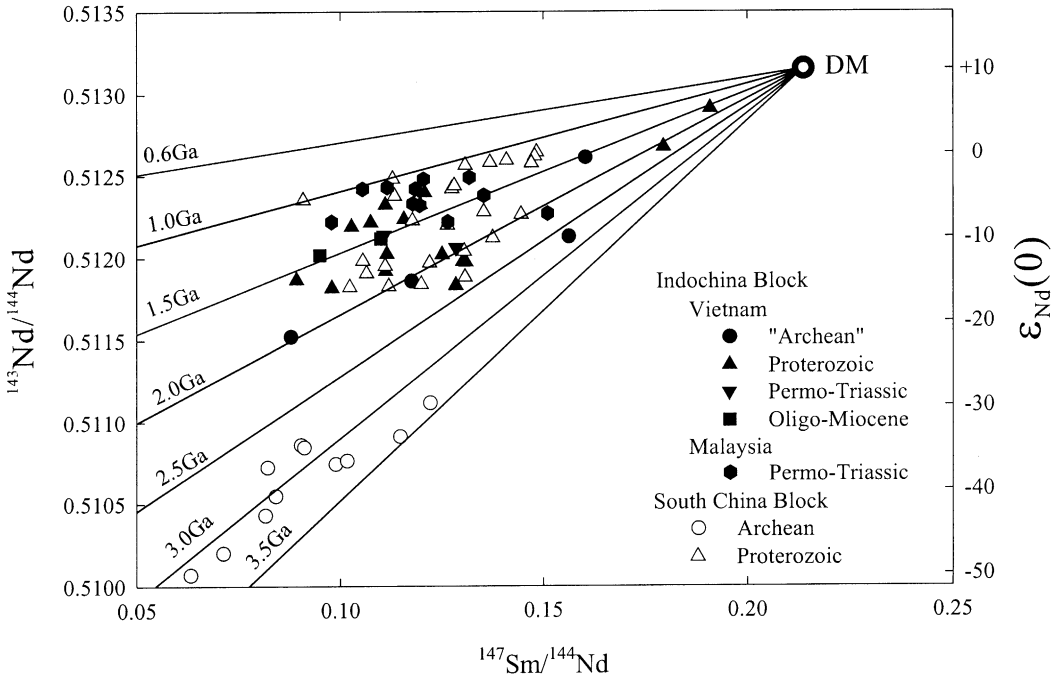

Fig. 6. Present day Sm–Nd isotopic data of Indochina block showing the "Archean" and Proterozoic basement rocks and Permo-Triassic charnockite of the Kontum massif, central Vietnam. Oligo-Miocene granitoids of Bu Khang complex (Nagy et al., 2000) in central Vietnam, Permo-Triassic granitic plutons of East Coast Province, Peninsular Malaysia (T_{DM} ages are recalculated, Liew and McCulloch, 1985) and basement rocks of South China block are shown for comparison. Data sources for South China block: Archean: Cavinh complex of northern Vietnam (Lan et al., 2001) and Kongling complex of China (Gao et al., 1999; Qiu et al., 2000); Proterozoic: Ailao Shan—Red River shear zone (Zhai et al., 1990; Zou et al., 1997; Zhang and Schärer, 1999; Lan et al., 2001). Nd model ages, assuming depleted mantle sources (DM), can be calculated from the slope of the tie lines connecting DM and any individual data point. Seven reference lines corresponding to model ages of 0.6, 1.0, 1.5, 2.0, 2.5, 3.0 and 3.5 Ga are shown.

of northern Yangtze (Gao et al., 1999; Qiu et al., 2000)), and Proterozoic rocks from the Ailao Shan—Red River shear zone (Zhai et al., 1990; Zou et al., 1997; Zhang and Schärer, 1999; Lan et al., 2001). All the rocks can be divided into two groups. Group I consists of rocks from central Vietnam and includes all the basement rocks and charnockites from this study and Oligo-Miocene granitoids of the Bu Khang complex, Permo-Triassic granitic rocks of Malaysia and Proterozoic basement rocks of the South China block. Group I is characterized by high $\varepsilon_{Nd}(0)$ values (−21.8 to +0.7) and essentially Proterozoic T_{DM} ages (1.0–2.4 Ga, except one 2.7 Ga). Group II, consisting of the Archean basement rocks of the South China block, shows very low $\varepsilon_{Nd}(0)$ values (−50 to −29.6) and middle to late Archean T_{DM} ages (2.7–3.5 Ga). In this regard, the basement rocks from central Vietnam are remarkably different from the Archean rocks from the South China block. So far no U–Pb dates older than 2.7 Ga have been reported for rocks from Vietnam, except some latest Archean ages for inherited zircon separates from the Kontum massif (2.7 Ga, Nagy et al., 2001; 2541 ± 55 Ma, Chung et al., unpublished data) and the Bu Khang area (2541 ± 69 Ma, Carter et al., 2001). Hence, the crust in central Vietnam appears to contain only insignificant amounts of recycled Archean rocks.

Proterozoic T_{DM} ages are also observed in the East Coast Province batholiths of the Peninsular Malaysia (Liew and McCulloch, 1985), located in the southwestern part of the Indochina block (Metcalfe, 2000). As shown in Fig. 6, the T_{DM} ages (mostly 1.0–1.6 Ga) for plutons from the East Coast Province of Malaysia are similar to the young T_{DM} ages characteristic of some of the rocks from central Vietnam in Group I. Zircon inheritance ages of the same province in

Malaysia also show younger ages (800 and 1350 Ma; Liew and McCulloch, 1985) than those of rocks of central Vietnam. Thus, the consistent and dominant Proterozoic T_{DM} ages of Indochina block suggest that the role of Archean rocks in the crustal evolution of Indochina block is limited. The main crust formation in the Indochina block was in the Proterozoic.

The Nd isotopic evolution in the constituent rocks of the Indochina block is illustrated in Fig. 7. According to the $\varepsilon_{Nd}(0)$ values and T_{DM} ages, two main crust-forming stages can be delineated. The first stage (solid lines in Fig. 7) is represented by the formation of the protoliths of the Kannack, Song Ba and Song Re complexes of Kontum massif. The ultimate sources of these rocks may have Paleoproterozoic ages, probably between 2.4 and 1.8 Ga. The second stage (dotted lines in Fig. 7) is manifested by the formation of the protoliths of the basement rocks of Kham Duc, Tu Mo Rong, Tak Po and Dieng Bong complexes of the Kontum massif during Paleoproterozoic to Mesoproterozoic time (2.1–1.2 Ga). The Phanerozoic (Paleozoic, Indosinian and Tertiary) magmatic rocks, consisting of intermediate to acidic lithologies, are plotted in the evolutionary trend defined by the two suits of basement rocks. This suggests that the Paleoproterozoic to Mesoproterozoic crusts were important sources for the Phanerozoic rocks.

The first stage rocks defined by the evolutionary trend (Fig. 7) were probably produced by remelting of the Paleoproterozoic (and/or late Archean) crustal materials. In this sense, mixing of the old crustal rocks with a substantial mantle input during Paleoproterozoic to Mesoproterozoic generated rocks of the second stage. The mantle input was most significant at ~450 Ma (Carter et al., 2001; Nagy et al., 2001), when rift-related magmatism occurred and thus caused mafic underplating in the lower crust, and eventually became the protolith of the amphibolites exposed during the Indosinian orogeny. In the meantime, the amphibolites served as the magma source for the charnockites, which were contaminated by crustal materials during ascent. The Indosinian orogeny furthermore resulted in a rapid, regional exhumation (Nam et al., 2001; Nagy et al., 2001) that brought the entire package

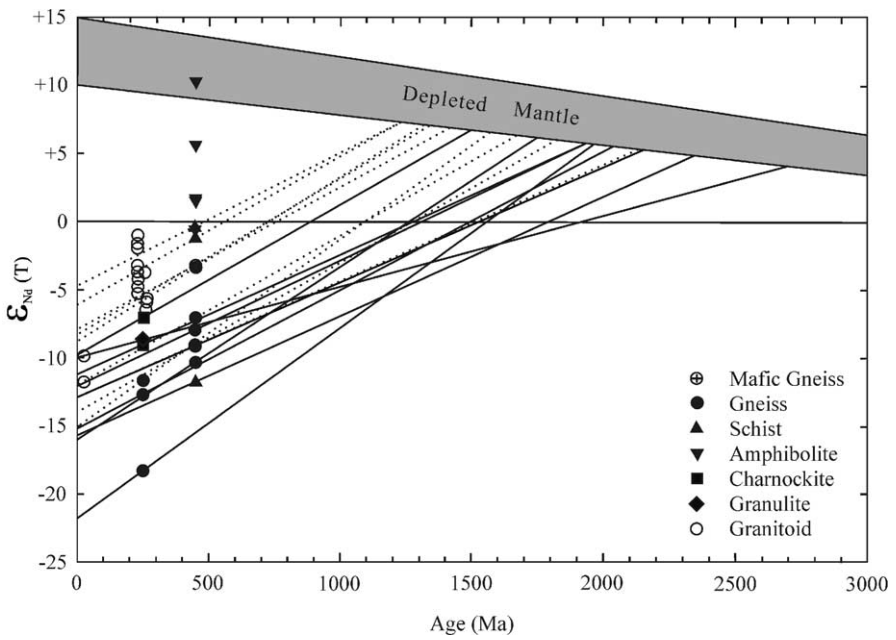

Fig. 7. Nd isotopic evolution diagram of igneous and metasedimentary rocks from the Indochina block. The solid lines represent the first crust-forming stage of basement rocks from Kannack, Song Ba and Song Re complexes. The dotted lines represent the second crust-forming stage of basement rocks from Kham Duc, Tu Mo Rong, Tak Po and Dieng Bong complexes. Data of granitoids (open symbols) are taken from Liew and McCulloch (1985) and Nagy et al. (2000). Others (solid symbols) are from this study.

of the Kontum basement rocks to the surface. By analogy, a significant mantle input has also been considered for generating the granitoids of the East Coast Province batholiths of Peninsular Malaysia (Liew and McCulloch, 1985) associated with the Indosinian orogeny along the western part of the Indochina block between 230 and 265 Ma.

6.2. Phanerozoic charnockites in the Indochina block

The origins (igneous versus metamorphic) of charnockites, a term first applied to hypersthene-bearing granites in India (Holland, 1900), have been the focus of much debate (Kilpatrick and Ellis, 1992). Therefore, it is important to determine whether the charnockites from the Kontum massif are of a metamorphic or igneous origin. These charnockites have basic to intermediate composition (Table 1). Two charnockites of this study, together with two charnockites from Nagy et al. (2001), show decreasing TiO_2, MgO, CaO and P_2O_5 with increasing SiO_2, which we interpret to be a fractionation trend. Fractionation may indicate crystallization of Ti-rich (e.g. ilmenite) and P-rich (e.g. apatite) phases. This inference is supported by the petrographic evidence for ilmenite and apatite. The decrease in Nb and Y with increasing SiO_2 can be interpreted by combined fractionation of ilmenite and apatite (Zhao et al., 1997). The development of small negative Eu anomalies with increasing SiO_2 may also result from apatite crystallization in addition to feldspar (Zhao et al., 1997). In addition, at a given SiO_2 content, these Vietnamese charnockites show relatively higher TiO_2 and P_2O_5, lower CaO (Fig. 8) and medium mg values (25–40) than those of metamorphic charnockites (Kilpatrick and Ellis, 1992). Thus, the geochemical and mineralogical features suggest a magmatic, rather than metamorphic, origin for the charnockites from the Kontum massif. Geochronological studies (Carter et al., 2001; Nam et al., 2001; Nagy et al., 2001) have shown that the charnockites formed during Indosinian time at

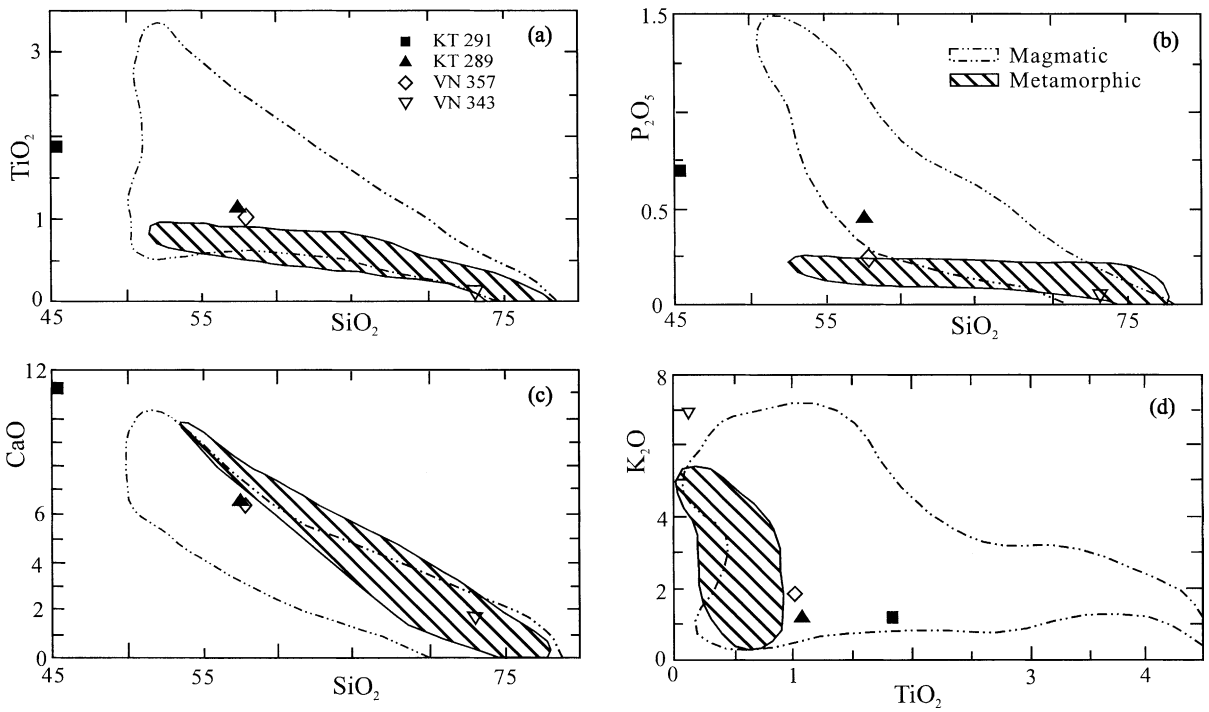

Fig. 8. Geochemical variation diagrams of the charnockites from the Kontum massif, central Vietnam. Solid symbols are of this study while open symbols are of Nagy et al. (2001). Also shown are the fields for magmatic and metamorphic charnockites of Kilpatrick and Ellis (1992).

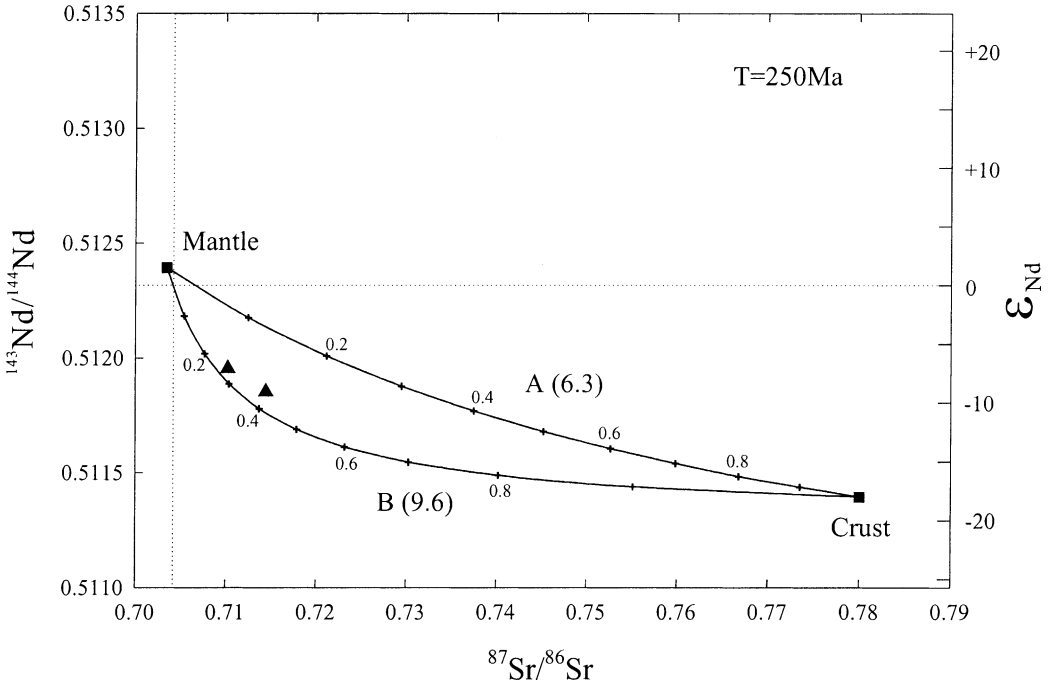

Fig. 9. Initial Nd and Sr isotopic composition for charnockites of the Kontum massif, central Vietnam at 250 Ma. Two-component mixing model was demonstrated with mantle ($\varepsilon_{Nd} = +1.5$, $^{87}Sr/^{86}Sr = 0.7035$) and crust ($\varepsilon_{Nd} = -18$, $^{87}Sr/^{86}Sr = 0.780$) as two end members. Two different mixing arrays are shown with varying concentration, for curve (A): mantle: [Sr] = 200 ppm, [Nd] = 6 ppm, crust: [Sr] = 240 ppm, [Nd] = 45 ppm; for curve (B): mantle: [Sr] = 650 ppm, [Nd] = 25 ppm, crust: [Sr] = 150 ppm, [Nd] = 60 ppm which corresponding to the curvature $[(Sr/Nd)_{mantle}/(Sr/Nd)_{crust}]$ of 6.3 and 9.6 for the hyperbola A and B, respectively. The concentrations of mantle and crust members for curve A are similar to those of TS22A and KT333/6, respectively, while those for curve B are similar to those of ocean island basalt (Wilson, 1988) and metapelite from high-grade metamorphic terranes (Prame and Pohl, 1994; Villaseca et al., 1998), respectively.

249 ± 2 to 258 ± 6 Ma. Thus, they represent one of the youngest (Phanerozoic) igneous charnockite terranes in the world (Nam et al., 2001).

The source rock composition for charnockites is controlled by numerous variables. The initial ε_{Nd} values i.e. ε_{Nd}(250 Ma), for the Kontum charnockites are −7.1 and −9.1, and can be interpreted as binary mixing (Fig. 9) between mantle-derived and crust-derived melts. The crustal end-member is proposed to have a composition similar to the gneiss KT333/6, which has the lowest ε_{Nd}(250 Ma) value (−18.3) and highest Sr isotopic ratio (0.7817). The mantle component is assumed to have a composition similar to the amphibolite TS22A, which has an ε_{Nd}(250 Ma) of +1.3 and chemical similarities to intraplate basalts. For simplicity, ε_{Nd}(250 Ma) value and initial Sr isotopic ratio for the crust end member are respectively chosen as −18 and 0.780, while those for the mantle are +1.5 and 0.7035. Two different mixing arrays (curves A and B), with different concentrations of Sr and Nd for the two end-members, are presented in Fig. 9. The curvatures of the two mixing lines, A and B, are represented by $(Sr/Nd)_{mantle}/(Sr/Nd)_{crust} = 6.3$ and 9.6, respectively. The two charnockites are bounded by the two assumed mixing curves. Although the Vietnamese charnockites are heterogeneous, the observed ε_{Nd}(250 Ma) range of the charnockites from the Kontum massif can be explained in terms of the mixing of mantle-derived (80–60%) and crust-derived (20–40%) melts using this simple calculation.

6.3. Crustal evolution of the Indochina block

T_{DM} age provides a constraint for the Precambrian crustal record of central Vietnam. The crustal history of Indochina block as revealed from central Vietnam

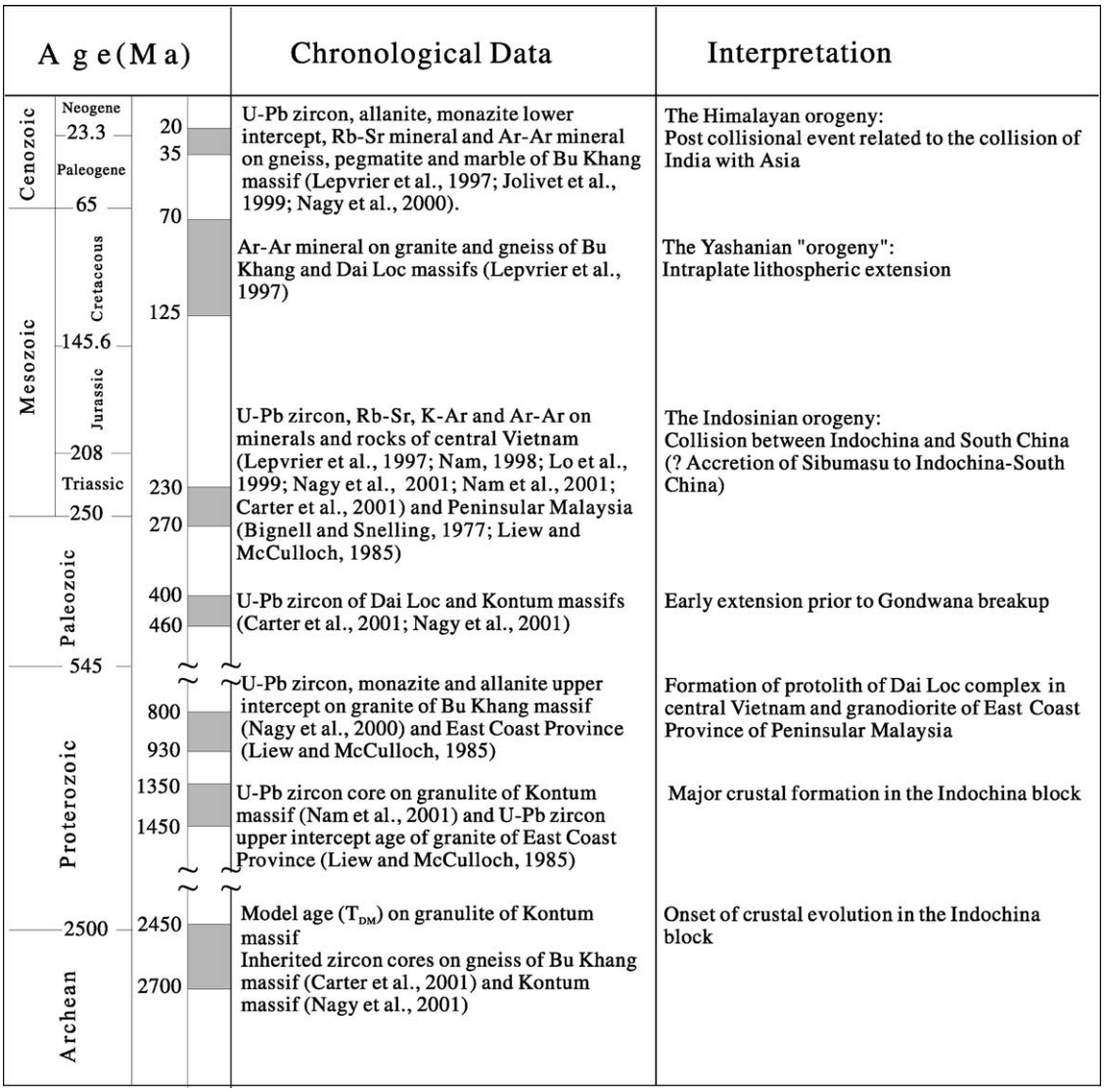

Fig. 10. Summary of major tectono-thermal events in Indochina block as reveal from central Vietnam and Peninsular Malaysia. Two samples of this study have been subjected to U–Pb zircon dating using SHRIMP which give five stages as 2541 ± 55, 1455 ± 24, 869 ± 57, 436 ± 10 and 260 ± 16 Ma (Chung et al., unpublished data).

and Peninsular Malaysia is summarized in Fig. 10. Nd model ages and U–Pb relict zircon or inherited zircon core ages (Carter et al., 2001; Nagy et al., 2001) suggest that continental crust of late Archean age (2.7–2.5 Ga) was separated from a depleted mantle and served as the source material for rocks of central Vietnam. At least two major crust formation stages have been delineated from T_{DM} ages (Fig. 7) for the Indochina block (Paleoproterozoic (2.4–1.8 Ga) and Mesoproterozoic (2.1–1.2 Ga)). So far, no reliable Paleoproterozoic dates have been obtained by U–Pb method. The Mesoproterozoic crust formation event has been registered in the zircon core of granulite sample of Kannack complex in the Kontum massif at 1404 ± 34 Ma using SHRIMP U–Pb dating (Nam et al., 2001) and U–Pb zircon upper intercept age of

~1350 Ma for adamellite of East Coast Province of Peninsular Malaysia (Liew and McCulloch, 1985). A Neoproterozoic event is presented by the upper intercept age of 881 ± 26 to 901 ± 26 Ma for zircon, allanite and monazite regression line from granitoid of Dai Loc pluton in central Vietnam (Nagy et al., 2000) and ~800 Ma for zircon from granodiorite of East Coast Province of Peninsular Malaysia (Liew and McCulloch, 1985). The T_{DM} ages in this study (which cover the rocks in the eastern part of Indochina block) and East Coast Province batholiths of Peninsular Malaysia (Liew and McCulloch, 1985) (which cover the rocks of the western part of Indochina block) are Mesoproterozoic instead of Neoproterozoic. We thus interpret the Mesoproterozoic event as the major crust formation event in the Indochina block, and the Neoproterozoic event is the magmatism for the formation of the protolith of Dai Loc complex in central Vietnam and the granodiorite of East Coast Province of Peninsular Malaysia. An early Paleozoic event has been identified from SHRIMP U–Pb zircon concordia ages of gneisses from the Dai Loc and Kontum massifs (407 ± 11 to 444 ± 17 Ma; Carter et al., 2001) and U–Pb zircon concordia ages of a granodiorite of Kontum massif (451 ± 3 Ma; Nagy et al., 2001). This event is most likely related to an extensional event that disintegrated the Indochina block from Gondwanaland (Carter et al., 2001). The magmatism produced the intraplate tholeiites, now represented by the amphibolites. Similar four age stages as 2541 ± 55, 1455 ± 24, 869 ± 57 and 436 ± 10 Ma (Chung et al., unpublished data) for sample KT318, reinforce the establishment of the Pre-Mesozoic crustal history.

The identification of 234 ± 5 to 260 ± 16 Ma high-grade metamorphism and charnockitic magmatism in central Vietnam (Lepvrier et al., 1997; Nam, 1998; Lo et al., 1999; Carter et al., 2001; Nam et al., 2001; Nagy et al., 2001; Chung et al., unpublished data) and K–Ar biotite age of 264 ± 7 Ma, Rb–Sr whole rock age of 261 ± 9 Ma (Bignell and Snelling, 1977) and U–Pb zircon lower intercept age of 257 ± 4 and 264 ± 2 Ma (Liew and McCulloch, 1985) for the granitic plutons in East Coast Province of Peninsular Malaysia suggest the Indosinian orogeny has affected the whole Indochina block. The fast cooling (~45 °C/Ma) and rapid exhumation (Nam et al., 2001) that occurred during this time exposed the high-grade basement rocks and charnockite of the Kontum massif. Using an intermediate value for the geothermal gradient (35 °C/km), this cooling rate suggests ~15 km of exhumation during a period of 12 Myr, corresponding to an average exhumation rate of ~1.3 mm per year. The Indosinian orogeny is a result of collision between the Indochina block and the South China block (Lepvrier et al., 1997; Chung et al., 1999; Lan et al., 2000, 2001). It caused a strong thermal overprinting (240–160 Ma, Lo et al., 1999) and exhumation of the Kontum massif. After suturing, both the Indochina and South China blocks may have experienced similar tectonothermal histories. Vestiges of the late Jurassic to Cretaceous Yanshanian "orogeny" and the mid-Tertiary Himalayan orogeny frequently found in the South China block have also left their traces in central Vietnam. The former is registered in the Truong Son belt, central Vietnam—a granite with age of 90.3 ± 0.7 Ma and mylonitic gneisses with increasing age spectra from 82 ± 10 to 130 ± 3 Ma using Ar–Ar muscovite dating (Lepvrier et al., 1997). The latter is recorded in U–Pb lower intercept dates (22.5 ± 1.7 to 26.0 ± 0.2 Ma) and Rb–Sr mineral dates (19.6 ± 0.5 to 21.2 ± 0.5 Ma) of granite (Nagy et al., 2000) and Ar–Ar mineral dating (21.4 ± 0.4 to 36.1 ± 1 Ma) of various metamorphic rocks (Lepvrier et al., 1997; Jolivet et al., 1999) from Bu Khang massif. However, there is no clear indication of thermal overprinting caused by the Cenozoic extrusion tectonics in the Kontum massif (Lo et al., 1999).

Acknowledgements

Dr. Nguyen Xuan Bao of Geological Survey Division No. 6, Vietnam is specially thanked for help with sample collection. We thank Y. S. Chia for preparing the figures, W. Y. Hsu and C. H. Chiu for analyzing the Sr, Sm and Nd isotopes and Y. Iizuka for mineral identification using probe analysis. The manuscript was improved by the comments of Kent C. Condie, Jian-xin Zhao and Zheng-Xiang Li and syntax polish of Cin-Ty Lee. This research was supported by Academia Sinica and the National Science Council of the Republic of China under grants NSC88-2116-M-001-034 and NSC89-2116-M-001-025 to C.Y. Lan. This paper is Contribution IESAS794 of the Institute of Earth Sciences, Academia Sinica.

References

Abbey, S., 1983. Studies in "standard sample" of silicate rocks minerals, 1969–1982. Geol. Surv. Canada Paper 83-15, pp. 1–114.

André, L., Deutsch, S., Hertogen, J., 1986. Trace element and Nd isotopes in shales as indexes of provenance and crustal growth: the early Paleozoic from the Brabant massif (Belgium). Chem. Geol. 57, 101–115.

Bao, N.X., Luong, T.D., Trung, H., 1994. Explanatory note to the geological map of Vietnam on 1:500,000 scale. Geol. Surv. Vietnam, Hanoi, 52 pp.

Bignell, J.D., Snelling, N.J., 1977. Geochronology of Malayan granites. Overseas Geol. Miner. Resources 47, Inst. Geol. Soc., London.

Boyd, F.R., Mertzman, S.A., 1987. Composition and structure of the Kaapvaal lithosphere, southern Africa: Magmatic processes: physicochemical principles (Edited by Mysen, B.O.). Geochem. Soc. Special Pub. 1, 13–24.

Carter, A., Roques, D., Bristow, C., Kinny, P., 2001. Understanding Mesozoic accretion in Southeast Asia: significance of Triassic thermotectonism (Indosinian orogeny) in Vietnam. Geology 29 (3), 211–214.

Chung, S.L., Lo, C.H., Lan, C.Y., Wang, P.L., Lee, T.Y., Hoa, T.T., Thanh, H.H., Anh, T.T., 1999. Collision between the Indochina and South China blocks in the Early Triassic: implications for the Indosinian orogeny and closure of eastern Paleo-Tethys: Eos (Trans., Am. Geophys. Union) 80 (46), F1043.

Department of Geology and Minerals of Vietnam (DGMVN), 1989. Geology of Vietnam: Stratigraphy, vol. 1. Science Publisher, Hanoi, 378 pp. (in Vietnamese).

Drummond, M.S., Defant, M.J., 1990. A model for trondhjemite-tonalite-dacite gneiss and crustal growth via slab melting: Archean to modern comparisons. J. Geophys. Res. 95, 21503–21521.

Gao, S., Ling, W., Qiu, Y., Lian, Z., Hartmann, G., Simon, K., 1999. Contrasting geochemical and Sm–Nd isotopic compositions of Archean metasediments from the Kongling high-grade terrain of the Yangtze craton: evidence for cratonic evolution and redistribution of REE during crustal anatexis. Geochim. Cosmochim. Acta 63 (13/14), 2071–2088.

Goldstein, S.L., O'Nions, R.K., Hamilton, P.J., 1984. A Sm–Nd isotopic study of atmospheric dusts and particulates from major river systems. Earth Planet. Sci. Lett. 70, 221–236.

Govindaraju, K., 1994. 1994 Compilation of Working Values and Sample Description for 383 Geostandards. Geostandards Newsletter 18 (Special Issue), 1–158.

Haskin, L.A., Wildeman, T.R., Frey, F.A., Collins, K.A., Keedy, C.R., Haskin, M.A., 1966. Rare earths in sediments. J. Geophys. Res. 71, 6091–6105.

Holland, T.H., 1900. The charnockite series, a group of Archean hypersthenic rocks in Peninsular India. Geol. Surv. India Mem. 28, 119–249.

Holtz, F., Barrey, P., 1991. Genesis of peraluminous granites. II. Mineralogy and chemistry of the Tourem complex (Northern Portugal)—sequential melting vs. restite unmixing. J. Petrol. 32, 959–978.

Humphris, S.E., Thompson, G., 1978. Hydrothermal alteration of oceanic basalts by seawater. Geochim. Cosmochim. Acta 42, 107–125.

Hutchison, C.S., 1989. Geological Evolution of Southeast Asia. Clarendon, Oxford, 368 pp.

Jolivet, L., Maluski, H., Beyssac, O., Goffé, B., Lepvrier, C., Thi, P.T., Vuong, N.V., 1999. Oligocene-Miocene Bu Khang extensional gneiss dome in Vietnam: geodynamic implications. Geology 27 (1), 67–70.

Katz, M.B., 1993, The Kannack complex of the Vietnam Kontum massif of the Indochina block: an exotic fragment of Precambrian Gondwanaland? In: Findlay, R.H., Unrug, R., Banks, M.R., Veevers, J.J. (Eds.), Gondwana 8. Rotterdam, Balkema, pp. 161–164.

Kilpatrick, J.A., Ellis, D.J., 1992. C-type magmas: igneous charnockites and their extrusive equivalents. Trans. R. Soc. Edinburgh, Earth Sci. 83, 155–164.

Lan, C.Y., Shen, J.J., Lee, T., 1986. Rb–Sr isotopic study of andesites from Lu-Tao, Lan-Hsu and Hsiao-Lan-Hsu: eruption ages and isotopic heterogeneity. Bull. Inst. Earth Sci. 6, 211–226.

Lan, C.Y., Chung, S.L., Shen, J.J., Lo, C.H., Wang, P.L., Hoa, T.T., Thanh, H.H., Mertzman, S.A., 2000. Geochemical and Sr–Nd isotopic characteristics of granitic rocks from northern Vietnam. J. Asian Earth Sci. 18, 267–280.

Lan, C.Y., Chung, S.L., Lo, C.H., Lee, T.Y., Wang, P.L., Li, H., Toan, D.V., 2001. First evidence for Archean continental crust in northern Vietnam and its implications for crustal and tectonic evolution in southeast Asia. Geology 29 (3), 219–222.

Lepvrier, C., Maluski, H., Vuong, N.V., Roques, D., Axente, V., Rangin, C., 1997. Indosinian NW-trending shear zones within the Truong Son belt (Vietnam): ^{40}Ar-^{39}Ar Triassic ages and Cretaceous to Cenozoic overprints. Tectonophysics 283, 105–127.

Li, X.-H., 1997. Geochemistry of the Longsheng Ophiolite from the southern margin of Yangtze Craton, SE China. Geochem. J. 31, 323–337.

Liew, T.C., McCulloch, M.T., 1985. Genesis of granitoid batholiths of Peninsular Malaysia and implications for models of crustal evolution: evidence from a Nd–Sr isotopic and U–Pb zircon study. Geochim. Cosmochim. Acta 49 (2), 587–600.

Lo, C.H., Chung, S.L., Lee, T.Y., Lan, C.Y., Wang, P.L., Long, T.V., Bao, N.X., 1999. Thermochronological study of the Kontum massif, central Vietnam and its implication to tectonothermal events in Indochina: Eos (Trans., Am. Geophys. Union) 80 (46), F1044.

Martin, H., 1986. Effect of steeper Archean geothermal gradient on geochemistry of subduction-zone magmas. Geology 14, 753–756.

Martin, H., 1994. The Archean gray gneisses and the genesis of continental crust. In: Condie, K.C. (Ed.), Archean Crustal Evolution. Elsevier, Amsterdam, pp. 205–260.

Masuda, A., Nakamura, N., Tanaka, T., 1973. Fine structures of mutually normalized rare earth patterns of chondrites. Geochim. Cosmochim. Acta 37, 239–248.

McLennan, S.M., 2001. Relationships between the trace element composition of sedimentary rocks and upper continental crust. G^3 (Electr. J. Earth Sci.), 2, April 20.

Mertzman, S.A., 2000. K–Ar results from the southern Oregon-northern California Cascade Range. Oregon Geol. 62 (4), 99–122.

Metcalfe, I., 1996. Gondwanaland dispersion, Asian accretion and evolution of eastern Tethys. Aust. J. Earth Sci. 43, 605–623.

Metcalfe, I., 1998. Paleozoic and Mesozoic geological evolution of the SE Asian region: multidisciplinary constraints and implications for biogeography. In: Hall, R., Holloway, J.D., Rosen, B.R. (Eds.), Biogeography and Geological Evolution of SE Asia. SPB Publishing, Amsterdam, pp. 25–41.

Metcalfe, I., 2000. The Bentong-Raub suture zone. J. Asian Earth Sci. 18, 691–712.

Miyashiro, A., 1974. Volcanic rock series in island arcs and active continental margins. Am. J. Sci. 274, 321–355.

Nagy, E.A., Schärer, U., Minh, N.T., 2000. Oligocene-Miocene granitic magmatism in central Vietnam and implications for continental deformation in Indochina. Terra Nova 12, 67–76.

Nagy, E.A., Maluski, H., Lepvrier, C., Schärer, U., Thi, P.T., Leyreloup, A., Thich, V.V., 2001. Geodynamic significance of the Kontum massif in central Vietnam: composite $^{40}Ar/^{39}Ar$ and U–Pb ages from Paleozoic to Triassic. J. Geol. 109, 755–770.

Nam, T.N., 1998. Thermotectonic events from early Proterozoic to Miocene in the Indochina craton: implication of K–Ar ages in Vietnam. J. Asian Earth Sci. 16 (5/6), 475–484.

Nam, T.N., Sano, Y., Terada, K., Toriumi, M., Van Quynh, P., Dung, L.T., 2001. First SHRIMP U–Pb zircon dating of granulites from the Kontum massif (Vietnam) and tectonothermal implications. J. Asian Earth Sci. 19, 77–84.

Prame, W.K.B.N., Pohl, J., 1994. Geochemistry of pelitic and psammopelitic Precambrian metasediments from southwestern Sri-Lanka: implications for two contrasting source-terrains and tectonic settings. Precambrain Res. 66, 223–244.

Qiu, Y.M., Gao, S., McNaughton, N.J., Groves, D.I., Ling, W., 2000. First evidence of >3.2 Ga continental crust in the Yangtze craton of south China and its implications for Archean crustal evolution and Phanerozoic tectonics. Geology 28, 11–14.

Reichen, L.E., Fahey, J.I., 1962. An improved method for the determination of FeO in rocks and minerals including garnet. US Geol. Surv. Bull. 1144B, 1–5.

Rogers, J.J.W., Greenberg, J.K., 1990. Late-orogenic, post-orogenic and anorogenic granites: distinction by major-element and trace element chemistry and possible origins. J. Geol. 98, 291–309.

Shen, J.J., Yang, H.J., Lan, C.Y., Chen, C.H., 1993. The setting up of isotope dilution mass spectrometry for REE analysis. J. Geol. Soc. China 36, 203–221.

Sun, S.S., McDonough, W.F., 1989. Chemical and isotopic systematics of oceanic basalts: implications for mantle composition and processes. In: Sanders, A.D., Norry, M.J. (Eds.), Magmatism in the Ocean Basins, Geol. Soc. London, Spec. Publ. 42, pp. 313–345.

Thanh, T.D., Janvier, P., Phuong, T.H., 1996. Fish suggests continental connections between the Indochina and South China blocks in Middle Devonian time. Geology 24, 571–574.

Tien, P.C. (Editor-in-chief), 1991. Geology of Cambodia, Laos and Vietnam: explanatory note to the geological map of Cambodia, Laos and Vietnam at 1:1,000,000, 2nd ed. Geological Survey of Vietnam, Hanoi, 158 pp.

Villaseca, C., Barbero, L., Rogers, G., 1998. Crustal origin of Hercynian peraluminous granitic batholiths of Central Spain: petrological, geochemical and isotopic (Sr, Nd) constraints. Lithosphere 43, 55–79.

Wilson, M., 1988. Igneous Petrogenesis. Unwin Hyman, London, p. 466.

Winchester, J.A., Floyd, P.A., 1977. Geochemical discrimination of different magma series and their differentiation products using immobile elements. Chem. Geol. 20, 325–343.

Zhai, M.G., Cong, B.L., Qiao, G.S., Zhang, R.Y., 1990. Sm–Nd and Rb–Sr geochronology of metamorphic rocks from SW Yunnan orogenic zones. China Acta Petrologica Sinica 6, 1–11 (in Chinese).

Zhang, L.S., Schärer, U., 1999. Age and origin of magmatism along the Cenozoic Red River shear belt. China Contrib. Miner. Petrol. 134, 67–85.

Zhao, J.X., Ellis, D.J., Kilpatrick, J.A., McCulloch, M.T., 1997. Geochemical and Sr–Nd isotopic study of charnockites and related rocks in the northern Prince Charles Mountains, East Antarctica: implications for charnockite petrogenesis and Proterozoic crustal evolution. Precambrian Res. 81, 37–66.

Zou, R., Zhu, B.Q., Sun, D.Z., Chang, X.Y., 1997. Geochronology studies of crust–mantle interaction and mineralization in the Honghe ore deposit zone. Geochimica 26, 46–56 (in Chinese).